Egypt. J. Chem. **Vol.** 68, SI: Z. M. Nofal, pp. 1247- 1263(2025)

Egyptian Journal of Chemistry

http://ejchem.journals.ekb.eg/

Utilization of Petroleum-Derived Waste Wax in Polyethylene Composites:A Sustainable Approach for Printing Ink Industry

Mohamed A. Amin*[a], Fathi S. Soliman [a], Fatma A. Morsy [C], Samya El Sherbiny [c] , Reem K. Farag [b], Nermen H. Mohamed[a]

[a]*Petroleum Refining Division, Egyptian Petroleum Research Institute, Cairo, Egypt*

[b]*Application Division, Egyptian Petroleum Research Institute, Cairo, Egypt*

[c]*Chemistry Department, Faculty of Science, Helwan University, Cairo, Egypt*

Abstract

The printing ink industry confronts considerable hurdles in balancing cost-effectiveness with sustainability, particularly when acquiring high-performance additives such as polyethylene wax. Our research offers a sustainable, cost-effective composite made from petroleum byproduct waste wax and high-Tg polymers (LDPE or HDPE), designed to replace traditional polyethylene wax. This composite solves both economic and environmental concerns by utilizing industrial waste while addressing the severe thermal, mechanical, and chemical requirements of ink formulations. The composite's uniform shape, crystallinity, and stability were confirmed through extensive thermal and structural characterization using differential scanning calorimetry (DSC), thermogravimetric analysis (TGA), X-ray diffraction (XRD), and scanning electron microscopy (SEM). The optimized formulation has a melting point of 88.5°C, a hardness of 3 mm, and thermal stability up to 90°C, which roughly matches commercial benchmarks.

When mixed into flexographic inks, the composite displays outstanding dispersion, near-comparable gloss (5% reduction), and abrasion resistance akin to normal waxes. Economic analysis shows a 34% reduction in material prices, demonstrating its industrial viability. This idea corresponds with UN Sustainable Development Goals (SDGs) 9 and 12, which promote circular economy concepts by repurposing garbage into a high-value resource. The study not only provides a competitive alternative in the printing industry, but it also establishes a scalable framework for developing sustainable materials in industries that rely on high-performance wax composites. This strategy highlights the intersection of economic success and environmental responsibility, paving the way for greener manufacturing models.

Keywords: macrocrystalline wax, microcrystalline wax, low-density polyethylene, high-density polyethylene, polymer/wax blend, rub resistance, flexographic ink.

1. Introduction

The growing demand for sustainable manufacturing practices has fuelled the search for environmentally friendly, cost-effective materials that adhere to circular economy principles and the United Nations Sustainable Development Goals (SDGs), particularly SDG 9 (Industry, Innovation and Infrastructure) and SDG 12 (Responsible Consumption and Production). In the printing ink industry, wax additives play a pivotal role in enhancing surface functionality, abrasion resistance, and slip performance. However, conventional synthetic waxes—notably polyethylene (PE) and polytetrafluoroethylene (PTFE)-are derived from fossil fuels, exhibit environmental persistence, and incur high production costs, rendering them unsustainable for high-volume, price-sensitive applications such as newsprint and magazine inks [1].

Petroleum-derived byproduct waxes (e.g., paraffin and microcrystalline waxes) offer a promising alternative due to their abundance in refinery waste streams and low cost. Paraffin wax, also known as macrocrystalline wax, is a solid hydrocarbon matrix primarily composed of linear alkanes (C_{16}–C_{30}), with a narrow melting range (45–80 °C) and low molten-state viscosity. It also contains branched isoalkanes (C_{18}–C_{36}) and alkyl-substituted cycloalkanes, which contribute to its high crystallinity (>90%) and hydrophobicity. These structural features give paraffin wax excellent dielectric properties, chemical stability, and low thermal conductivity, making it widely applicable in packaging, coatings, cosmetics, and phase-change materials (PCMs) [2,3].

In contrast, microcrystalline waxes exhibit a microstructure consisting of submicron, entangled crystalline domains. Despite their crystalline nature, they are often considered amorphous due to their plastic deformation behaviour. These waxes are richer in isoalkanes, cycloalkanes, and alkylated aromatics, yielding enhanced flexibility, adhesiveness, and higher melting temperatures (60–95 °C) compared to paraffin wax. Their high molten-state viscosity and resistance to recrystallization make them particularly valuable in hot-melt adhesives, rubber modification, and corrosion-resistant

*Corresponding author e-mail: Mohamed.Amin94.3.4@gmail.com.(Mohamed A. Amin).

Received date 12 May 2025; revised date 03 August 2025; accepted date 16 August 2025

DOI: 10.21608/ejchem.2025.382623.11723

coatings [4,5].

Waste wax represents a significant untapped petroleum resource with high value-addition potential. As an abundant, low-cost byproduct of petroleum refining processes—generated globally at >2.5 million tons/year—it poses substantial environmental disposal challenges. Despite this promise, waste waxes exhibit critical limitations including poor dispersion stability, low hardness, incompatibility in polar ink matrices, and suboptimal thermal properties [5 - 7].

Paraffin wax/polymer composites have been widely explored to overcome the inherent limitations of unmodified waxes in demanding applications. Commonly used systems include paraffin wax blended with polyethylene (PE), ethylene-vinyl acetate (EVA), or polypropylene (PP), which improve flexibility, adhesion, and thermal resistance [8–10]. For instance, LDPE/paraffin composites are known to enhance film-forming properties and reduce wax brittleness, while HDPE additions can significantly increase hardness and elevate the melting point range beyond 100 °C [11, 12]. These composites exhibit enhanced compatibility with non-polar ink components and offer better rub resistance than neat waxes. However, a critical review of the literature reveals that the vast majority of these studies utilize virgin-grade waxes and polymers, focus on generic material properties (e.g., melting point, tensile strength), and are rarely directed toward specific industrial applications, particularly in printing technologies.

Furthermore, there is a lack of systematic correlation between composite microstructure and its functional performance, especially in relation to ink formulation requirements such as dispersibility, film-forming behavior, and surface durability. Additionally, economic and environmental evaluations of such composite systems are seldom addressed, despite their importance for commercial-scale adoption.

Recent initiatives aimed at the valorisation of industrial waste have highlighted the latent potential of petroleum refining byproducts. However, their broader application remains constrained by inherent material limitations. It is widely recognized that the non-rubbing properties of waxes are strongly influenced by key physicochemical factors such as particle size, hardness, and melting temperature [13].

To address these limitations, this study proposes a sustainable modification strategy involving the blending of waste petroleum waxes with polymers to enhance their thermal stability, hardness, and dispersion characteristics. Specifically, high-performance composite formulations were developed by incorporating low-density and high-density polyethylene (LDPE and HDPE) into Paraffin and microcrystalline wax matrices.Through optimization of blend ratios and advanced characterization techniques—including differential scanning calorimetry (DSC), thermogravimetric analysis (TGA), and scanning electron microscopy (SEM)—improvements in thermal stability, crystallinity, and dispersion behaviour in flexographic ink systems were achieved. The proposed approach leverages polymer–wax miscibility to tailor morphological features, thereby enhancing rub resistance, substrate adhesion, and overall thermal performance—functional properties that are unattainable with unmodified petroleum waxes [14,15].

Through a direct performance comparison with conventional PE waxes, our composite systems demonstrate improved dispersion stability, higher thermal degradation temperatures (by > 15 °C), and greater surface uniformity under SEM imaging. These enhancements directly correlate with improved print quality and durability in flexographic ink systems. By integrating underutilized refinery byproducts into functional wax polymer blends, this work presents a scalable and sustainable alternative to petroleum based commercial waxes, reinforcing the economic and ecological value of the proposed solution [16].

Economically, the prepared paraffin and microcrystalline wax/polymer composites offer a significant cost advantage over conventional PE waxes. Waste refinery waxes—typically priced at 20–40% of the cost of synthetic waxes—are widely available but underutilized due to disposal and compatibility challenges [16]. By incorporating these low-cost byproducts with polymers, the composite systems reduce raw material costs, avoid energy-intensive synthesis, and support sustainable material vaporization. This makes them ideal for adoption in large-scale, cost-sensitive applications like ink formulations, packaging, and coatings.

This study aims to develop and optimize paraffin wax/polymer composites using petroleum oil byproduct waste wax, targeting performance standards for the printing ink industry. The primary objectives are to:

1. Enhance the thermal, mechanical, and chemical properties of waste wax *via* blending with high T_g polymers (e.g., LDPE and HDPE)
2. Achieve performance comparable or superior to commercial polyethylene (PE) waxes in melting temperature, hardness, and ink formulation compatibility including rub resistance and thermal behavior relevant to press performance.
3. Evaluate the economic viability and environmental impact of waste wax utilization, aligning with UN Sustainable Development Goals (SDGs) 9 (Industry, Innovation, and Infrastructure) and 12 (Responsible Consumption and Production).

Addressing these objectives will deliver a cost-effective, environmentally sustainable alternative for the printing ink industry, with potential extensibility to high-performance wax composite applications.

2. Materials and Methods

2.1. Materials

Macrocrystalline wax was derived from heavy slack wax supplied by El-Ameria Petroleum Refining Company (Alexandria, Egypt). It exhibited a melting point of 68 °C, purity ≥ 98 wt%, and was used without further purification.

Microcrystalline wax was obtained from crude petrolatum, sourced from Alexandria Petroleum Company (Alexandria, Egypt), with a melting point of 78 °C and purity ≥ 95 wt%.

High-density polyethylene (HDPE) pellets were procured from ExxonMobil Chemical Company (Houston, TX, USA). The HDPE had a melt flow index (MFI) of 19 g/10 min (measured at 190 °C/2.16 kg, ASTM D1238), a weight-average molecular weight (Mw) of 298,615 g/mol, melting point of 130 °C, density of 0.95 g/cm³, and purity ≥ 99 wt%.

Low-density polyethylene (LDPE) pellets were also supplied by ExxonMobil Chemical Company (USA), with a melt flow index of 22.0 g/10 min (ASTM D1238), a weight-average molecular weight of 309,065 g/mol, melting point of 102 °C, density of 0.918 g/cm³, and purity ≥ 99 wt%.

Micronized wax additive (mju: wax® 2002 FN) was obtained from Ceronas GmbH & Co. KG (Kitzingen, Germany). This synthetic wax additive had a melting point of 110 °C, needle penetration hardness of 3 mm (ASTM D1321), density of 0.95 g/cm³ at 23 °C, and a particle size distribution of D50 = 8 µm and D99 = 22 µm (measured via laser diffraction). Purity was specified by the manufacturer as ≥ 99.5 wt%.

Flexographic cyan ink, specifically formulated for polyethylene film printing, was sourced from J-Pack Company (Cairo, Egypt). The ink contained pigment blue 15:3, a Nitrocellulose resin, and solvent blends.

2.2. Methods

2.2.1 Preparation of wax blends

High-density polyethylene (HDPE) and low-density polyethylene (LDPE) pellets were melted separately at 160°C and 140°C, respectively. Each melted polyethylene (PE) was combined with either macrocrystalline wax (68°C melting point) or microcrystalline wax (78°C melting point) in a mechanical stirrer at 100 rpm for 30 min. Blends were formulated at wax/PE weight ratios of 50/50, 60/40, 70/30, and 80/20 (w/w).

For HDPE-based blends, the mixtures were melt-pressed at 160°C under 90 bar pressure for 5 min using a hot-melt press; LDPE-based blends were pressed at 140°C under identical pressure and duration. The resulting films were subsequently ground into fine powder via a ball mill (stainless steel balls, 500 rpm, 1 h).

2.2.2 Ink Formulations

A solvent-based cyan flexographic ink formulation (Table 1) was selected to evaluate wax/polymer blend efficacy. Four ink variants were formulated in collaboration with J-Pack Company (Egypt):

Table 1: displays the components found in the commercially available cyan ink

Ingredients	Function		Amount % w/w
Carbon black	Pigment		15.00
Nitrocellulose	Resin		15.00
Ethanol	Solvent		40.00
ethyl acetate			27.00
Dispersing agent	Additives	For pigment dispersion	1
Wax		for Rub resistance	2

(a) a wax-free control ink;
(b) a comparative ink containing commercial mju: wax® 2002FN;
(c) experimental wax/polyethylene blends at 50:50, 60:40, 70:30, and 80:20 ratios.

2.3 Characterization of the wax blends

An SDTQ 600 thermal and thermogravimetric analyzer (TA-USA) was utilized to conduct both differential scanning calorimetry (DSC) and thermogravimetric analysis (TGA) on high-melting-point macro- and micro-crystalline waxes, as well as low-density polyethylene (LDPE), high-density polyethylene (HDPE), and their mixtures. DSC measurements were performed within a temperature range of 25–180°C at a heating rate of 5°C/min, while TGA assessments were performed from 25 to 700°C at a heating rate of 10°C/min under a dynamic nitrogen atmosphere. The objective of these analyses is to assess the thermal characteristics and stability of the materials.

X-ray diffraction patterns were acquired for high-melting-point macrocrystalline and microcrystalline waxes, along with their LDPE and HDPE composites, using a Philips Analytical X-ray diffractometer. Patterns were recorded over a 2θ range of 4–79° with a step size of 0.03° (2θ) and a counting time of 0.6 s per step. Measurements employed Cu $K\alpha_1$ radiation (λ = 1.54060 Å) at 40 kV, with parallel-beam incident angle fixed at 0.02° (2θ). Crystallinity was quantified by calculating the ratio of the integrated area under Bragg diffraction peaks to the total area (Bragg peaks + amorphous halo).

Penetration measurement is the predominant method for assessing the hardness and thermal behaviour of petroleum waxes. This technique quantifies the depth to which a standardized needle or cone penetrates a wax sample under specified conditions. In this study, hardness was determined via needle penetration (ASTM D-1321 method) for firmer wax grades using a digital precision penetrometer.

The congealing temperature was established in accordance with the ASTM D938-12 guidelines. In summary, a wax sample was melted and a small amount was attached to the bulb of the thermometer. The droplet on the bulb was then cooled at a constant rate using a pre-warmed flask as an air jacket until it solidified. The congealing temperature was determined as the point at which the droplet stopped flowing when the thermometer was rotated.

2.4 Characterization of the prepared inks

The test ink formulations incorporating modified petroleum wax were evaluated for slip, gloss, and rub resistance properties. Rub resistance was quantified by measuring the printed sample's durability against sustained surface friction, following ASTM D5264 methodology. Testing involved reciprocating an abrasive material against the printed substrate for 150 cycles under 4 lb (1.8 kg) applied pressure. Damage assessment was performed via visual inspection using a Labthink Ink Rub Tester RT-01.

Slip refers to the resistance against relative motion between contacting surfaces. This property was quantified using a Labthink MXD-02 coefficient of friction tester by progressively *inclining* a plane containing two interfaced specimens until sliding initiation occurred.

Gloss, influenced by ink composition, substrate characteristics, and film surface topography, was measured by directing collimated light at a standardized angle (typically 60°) onto the ink film and quantifying the secularly reflected light intensity. This reflection percentage correlates directly with perceived surface gloss, as determined using a TQC Sheen glossmeter.

To conduct these tests, various drawdowns were prepared using the test ink formulations. This included a control formulation without any wax additives, commercially available wax (mju: wax® 2002 FN), or custom wax blends. These drawdowns were applied to Form 3NT-3 Coated Book Leneta Test Sheets using a #6 Meyer rod. Following the application, the samples were dried in an oven for 30 s at 60 ºC and subsequently left at room temperature for 24 h prior to testing.

3. Results and discussion

3.1. Analysis of the formulated wax mixtures

3.1.1. Differential scanning calorimetry (DSC)

Figures 1- 4 illustrate the DSC curves for LDPE, HDPE, macro-and microcrystalline waxes, and blends of LDPE and HDPE that include 50, 60, 70, and 80 wt percent of either macro-or microcrystalline wax. The DSC outputs revealed three distinct peaks, where the exhibit similar thermal characteristics because of the absence of chemical reactions between the waxes and polymers [17]. The results indicate that both macrocrystalline and microcrystalline waxes were successfully blended with LDPE and HDPE. The enthalpy of fusion (ΔH_m) was determined by integrating the total area under the DSC peaks corresponding to solid–solid and solid–liquid transitions for both wax types within the composites. This numerical integration approach enabled the quantification of crystallinity variations in the blends, which were found to be dependent on the ratio of macro- to microcrystalline waxes. These findings are consistent with established methodologies for assessing crystallinity in polymer–wax systems [18].

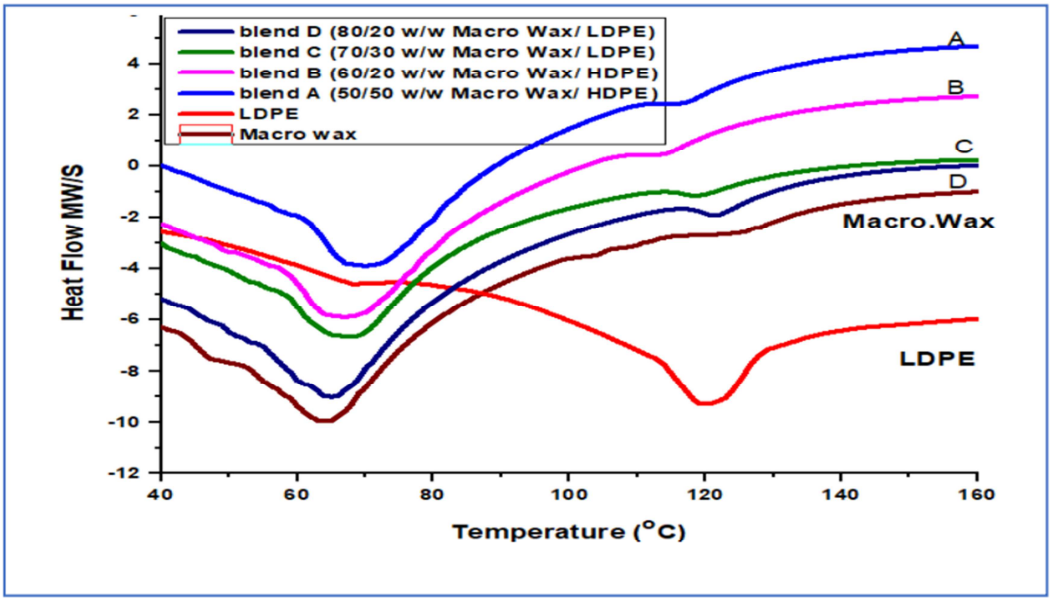

Figure 1 DSC curves of LDPE, macrocrystalline wax, and macrocrystalline wax/LDPE.

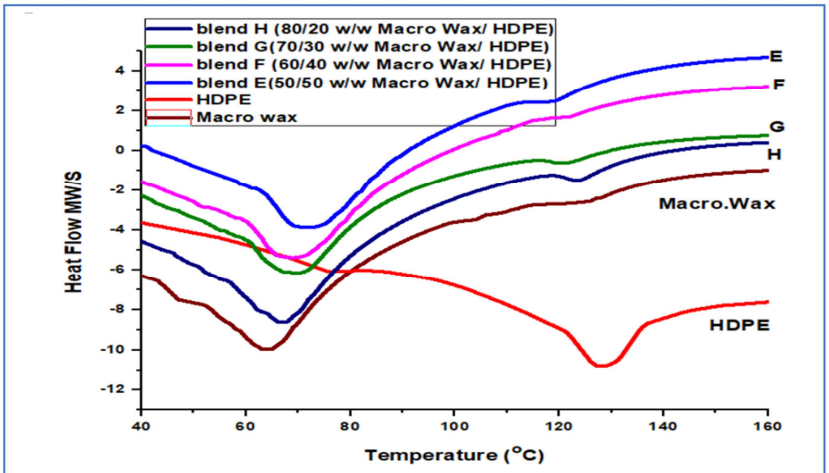

Figure 2 DSC curves of LDPE, macrocrystalline wax, and Macrocrystalline wax/HDPE.

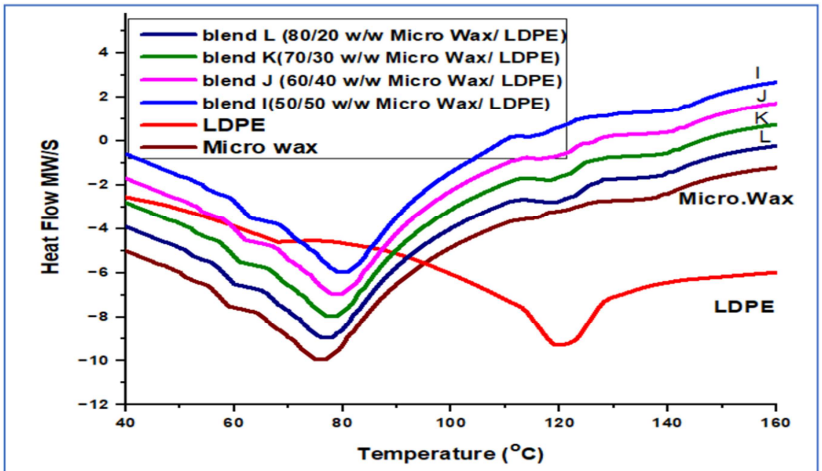

Figure 3 DSC curves of LDPE, Microcrystalline wax, and Microcrystalline wax/LDPE

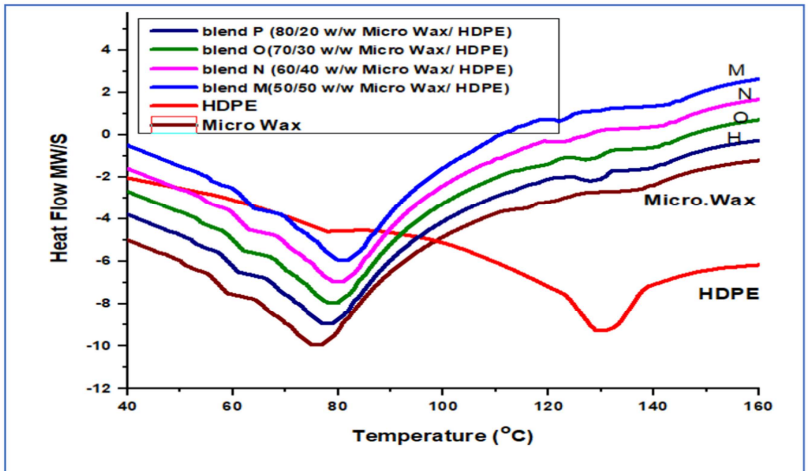

Figure 4 DSC curves of LDPE, Microcrystalline wax, and Microcrystalline wax/HDPE

The thermal properties of pure waxes, along with the combinations of macro- and micro-crystalline waxes with LDPE and HDPE, are summarized in Tables 2 and 3. This includes key metrics such as transition temperature (Tt), melting temperature (Tm), and melting enthalpy (ΔHm) as measured by the DSC thermal Analyzer.

Tt and Tm of the blends decreased systematically with reduced polymer content (Tables 2 and 3). For instance, macrocrystalline wax/LDPE blends (50/50 to 80/20), Tt declined from 63.52°C to 58.72°C, while Tm decreased from 88.45°C to 74.41°C. This trend aligns with the plasticizing effect of molten wax, which disrupts polymer chain packing and lowers thermal stability [17]. A parallel reduction in Tt and Tm was observed in HDPE-based blends, though with higher absolute values due to HDPE's inherently greater crystallinity. The enthalpy of fusion (ΔHm) for wax components exhibited an inverse relationship with polymer concentration. As polymer content decreased from 50 to 20 wt%, ΔHm for macrocrystalline wax/LDPE blends increased from 10.8 to 12.4 cal/g, while macrocrystalline wax/HDPE blends showed. rise from 10.2 to 11.4 cal/g. Similarly, microcrystalline wax blends demonstrated comparable trends (e.g., ΔHm increased from 10.5 to 12.2 cal/g for HDPE blends). These results indicate enhanced wax crystallinity at lower polymer ratios, stemming from reduced polymer-induced confinement of crystallization domains. Notably, macrocrystalline wax exhibited more pronounced crystallinity enhancement than microcrystalline wax, indicating greater susceptibility to polymer-induced lattice distortion [18].

XRD analysis corroborated these findings; with macrocrystalline wax/HDPE blends (80/20) achieving 70% crystallinity compared to 63% for equivalent LDPE blends. This disparity underscores HDPE's superior ability to preserve wax crystallinity, likely due to its higher initial crystallinity and structural compatibility with wax phases [17]. The total enthalpies of HDPE-based blends (e.g., 12.8 cal/g for macrocrystalline/HDPE vs. 12.4 cal/g for macrocrystalline/LDPE) further highlight this distinction.

Crystallinity compared to that of microcrystalline wax. This implies that LDPE and HDPE have a more significant impact on the distortion of the crystal lattice of the macrocrystalline wax.

Table 2: The onset and peak temperatures, along with the melting enthalpies, of the Macro-crystalline wax samples examined through DSC

Sample	T_t (°C)	T_m (°C)	ΔH_m (cal/g)	Crystallinity (%)
Macro-crystalline wax/LDPE				
100/0	56.8	68.53	27.8	84
50/50 (Blend A)	63.52	88.45	10.8	63
60/40 (Blend B)	61.72	77.85	11.4	63
70/30 (Blend C)	60.02	76.05	11.7	65
80/20 (Blend D)	58.72	74.41	12.4	70
Macro-Crystalline Wax/HDPE				
50/50 (Blend E)	64.32	89.65	11.2	64
60/40 (Blend F)	62.79	78.8	11.8	65
70/30 (Blend G)	61.42	77.25	12.1	67
80/20 (Blend H)	59.82	75.51	12.8	72

Table 3: DSC onset and peak temperatures and melting enthalpies of the microcrystalline wax samples examined through DSC

Sample	Tt (°C)	T_m (°C)	ΔH_m (cal/g)	Crystallinity (%)
Micro-crystalline wax/LDPE				
100/0	62.29	78.83	29.7	63
50/50 (Blend I)	69.72	84.45	10.2	61
60/40 (Blend J)	68.92	83.85	10.4	61
70/30 (Blend K)	67.72	82.45	10.7	62
80/20 (Blend L)	66.32	81.41	11.4	62
Micro-crystalline wax/HDPE				
50/50 (Blend **M**)	70.22	84.95	10.5	61
60/40 (Blend **N**)	69.42	84.25	10.9	61
70/30 (Blend **O**)	68.32	82.95	11.6	62
80/20 (Blend **P**)	66.92	81.81	12.2	62

Crystallinity Percentage -XRD **(%)-** Used to quantify the **crystalline vs. amorphous content** in semi-crystalline materials like polymers, wax/polymer composites, cellulose, etc. the samples were estimated from the X-ray diffraction (XRD) patterns by separating the crystalline and amorphous contributions. The crystallinity index was calculated using the following equation:

$$\textbf{Crystallinity}\ \% = \frac{\mathrm{Ac}}{\mathrm{Ac} + \mathrm{Aa}} \times 100$$

- Ac: Area under crystalline peaks
- Aa: Area under amorphous hump

- Ac+Aa: Total area under the XRD curve

3.1.2. Thermogravimetric analysis TGA

Thermogravimetric analysis (TGA) was used to assess the thermal degradation behavior of macro- and microcrystalline wax blends with low- and high-density polyethylene (LDPE, HDPE) of various compositions. Figures 5-8 show the weight loss curves for different systems, exhibiting significant tendencies in thermal stability that is impacted by polymer type, wax structure, and mix ratios.

Macrocrystalline Wax Blends

For macrocrystalline wax blends, increasing LDPE or HDPE content markedly improved thermal stability (Figures 5–6). Pure LDPE and HDPE exhibited higher decomposition onset temperatures than pure wax, consistent with their inherent thermal resistance. Blends containing 50 wt% polymer showed elevated degradation onset temperatures, with HDPE-based systems outperforming LDPE counterparts. This performance differential stems from HDPE's greater molecular weight, crystallinity, and melting temperature—collectively enhancing matrix protection against thermal degradation [16]. Polyethylene lamellae likely shield less stable wax chains from premature decomposition, while wax-induced crystallinity elevation reinforces the polymer network [17,19]. Reducing polymer content from 50 to 20 wt% systematically lowered decomposition temperatures, indicating reduced protective capacity of the polymer phase.

The 35°C higher onset temperature in 50 wt% HDPE blends (vs. LDPE; Figure 5b) originates from HDPE's superior structural stability [16]. XRD analysis (Figure 9) confirms wax-induced polyethylene crystallinity enhancement (ΔXc = 18%), suggesting cooperative network formation [17,19]. At 20 wt% polymer, decreased lamellar continuity reduces this shielding effect, lowering onset temperatures by 22–29°C.

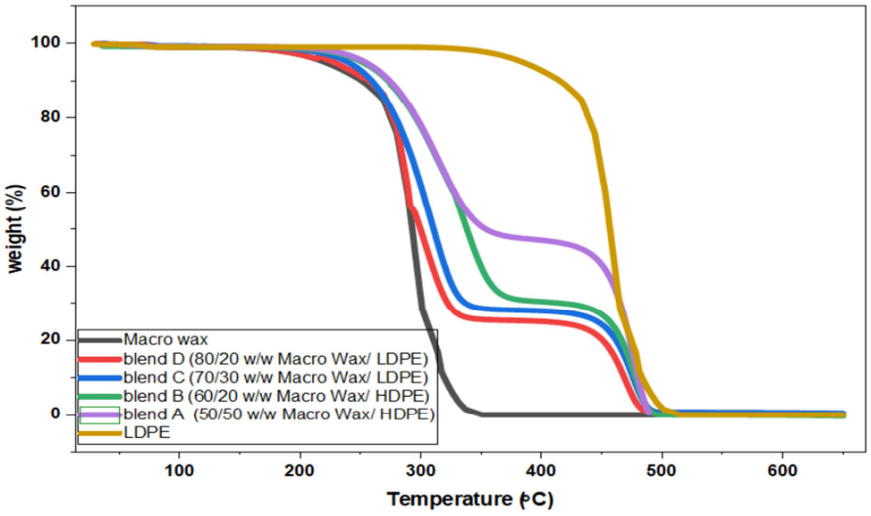

Figure 5: **TGA profiles of HDPE, macrocrystalline wax, macrocrystalline wax /LDPE Blends**

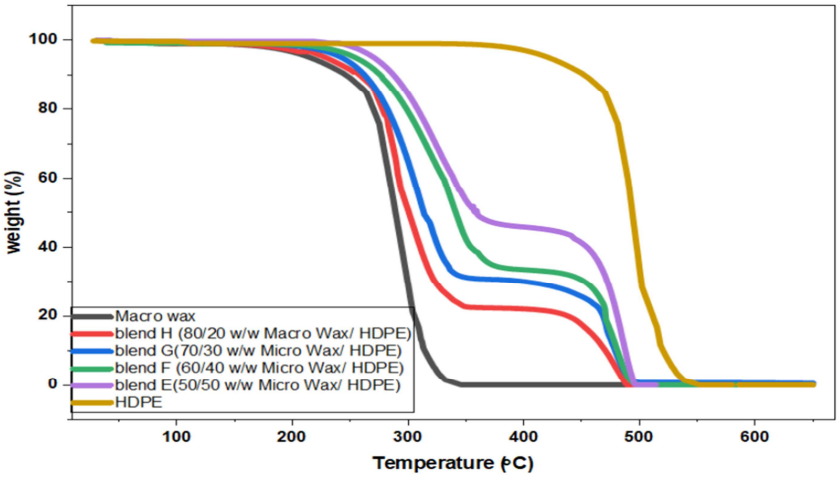

Figure 6: **TGA profiles of HDPE, macrocrystalline wax, macrocrystalline wax /HDPE Blends**

Microcrystalline Wax Blends

Similar trends occurred in microcrystalline wax blends (Figures 7–8), though with slightly reduced thermal stability relative to macrocrystalline counterparts. Microcrystalline wax/HDPE blends again demonstrated superior stability to LDPE-based systems, highlighting the critical role of polymer architecture. Given microcrystalline wax's smaller crystal domains and branched molecular structures, it integrates less effectively with polyethylene lamellae-yielding weaker interfaces and accelerated degradation under thermal stress, particularly at lower polymer loadings [5,6].

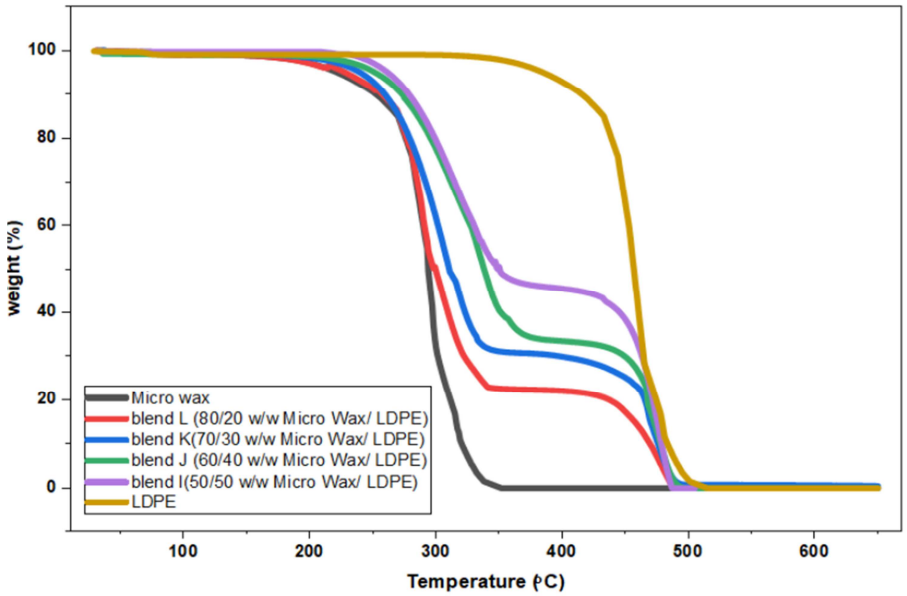

Figure 7: TGA profiles of LDPE, Microcrystalline wax, Microcrystalline wax/LDPE Blends

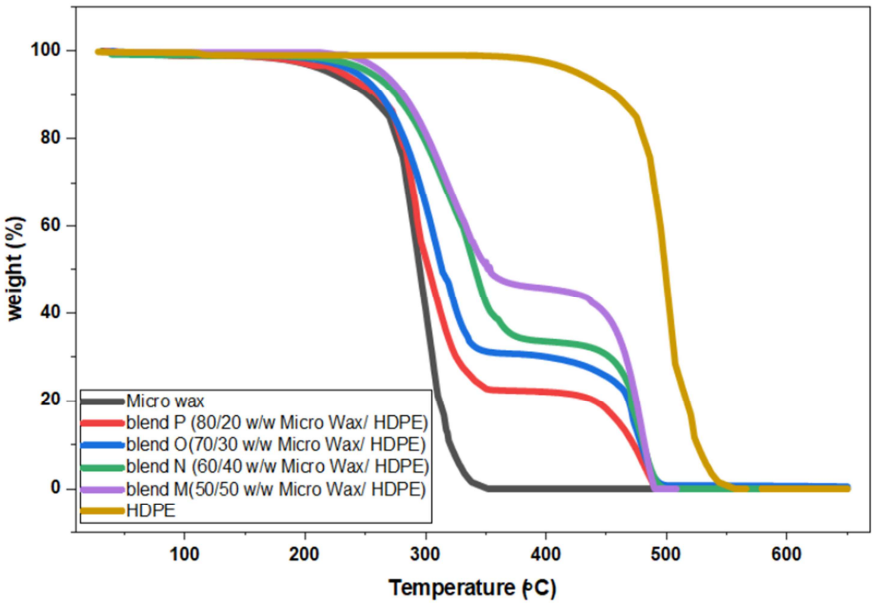

Figure 8: TGA profiles of HDPE, Microcrystalline wax, Microcrystalline wax/HDPE blends

The superior thermal resistance of HDPE blends, irrespective of wax type, underscores the critical role of polymer crystallinity and molecular weight in composite stabilization. At 500°C, macrocrystalline wax/HDPE (80/20 wt%) blends retained >70% residual mass, whereas equivalent LDPE blends preserved only ~65% (Figures 5–6). This differential originates from HDPE's enhanced capacity to maintain structural integrity under thermal stress, thereby delaying wax

Similar thermal behavior was observed in microcrystalline wax blends (Figures 7–8), albeit with slightly reduced thermal stability compared to their macrocrystalline counterparts. Among these, microcrystalline wax/HDPE composites consistently exhibited greater thermal resistance than LDPE-based systems, underscoring the influence of polymer architecture. Due to the branched molecular structure and smaller crystalline domains of microcrystalline wax, its integration with polyethylene lamellae is less efficient, resulting in weaker interfacial bonding and accelerated thermal degradation—particularly at lower polymer loadings [5,6].

The enhanced thermal resistance of HDPE-based blends, regardless of wax type, highlights the critical role of polymer crystallinity and molecular weight in stabilizing the composite. At 500°C, macrocrystalline wax/HDPE blends (80/20 wt%) retained over 70% of their original mass, whereas equivalent LDPE blends retained approximately 65% (Figures 5–6). This discrepancy is attributed to HDPE's superior structural integrity under thermal stress, which delays the volatilization of wax components. Notably, an inverse relationship was observed between polymer concentration and blend stability, suggesting that polymer-driven protective mechanisms govern degradation behavior.

HDPE's higher crystallinity (~70–85%) and linear chain structure, compared to LDPE (~40–60% crystallinity), promote the formation of more effective thermal barriers. As shown in Figure 6, the 15% increase in mass retention for HDPE blends at 500°C is attributed to reduced molecular mobility within ordered crystalline domains, which restricts the escape of low-molecular-weight wax fractions [20,21].

3.1.3. X-ray diffraction

The crystalline structure of macro- and microcrystalline waxes and their blends with low- and high-density polyethylene (LDPE, HDPE) was investigated via X-ray diffraction (XRD). Figures 9–12 illustrate the diffraction patterns for pure waxes and their blends at varying polymer ratios (50/50 to 80/20 wax/polymer).

Macrocrystalline Wax Blends

Pure macrocrystalline wax (Figure 9) shows three distinct peaks at 2θ = 21.6°, 23.95°, and 36.05°, indicating a well organized crystalline lattice (crystallinity: 84%; Table 2). Crystallinity dropped to 63% and 64%, respectively, when 50 wt% LDPE or HDPE was blended in, as demonstrated by reduced peak intensities and the depression of the 36.05° peak (Figures 9 and 10). This reduction in crystallinity is caused by polymer-induced disruption of wax crystal packing, when polyethylene chains intercalate into the wax matrix, decreasing long-range order [16].

Reducing polymer content from 50 to 20 wt% produced distinct crystallinity trends in LDPE and HDPE systems. In HDPE-based blends (Figure 10), crystallinity increased from 64% to 67%, attributed to HDPE's intrinsic stiffness and higher crystallinity, which promote partial reordering of wax domains. In contrast, LDPE blends (Figure 9) showed only a marginal increase in crystallinity (from 63% to 64%), a result of LDPE's branched molecular architecture that imposes greater steric hindrance, limiting the extent of wax recrystallization [22]. These findings align with DSC-derived enthalpy data (Table 2), highlighting the strong correlation between thermal and structural behavior in polyethylene–wax composites.

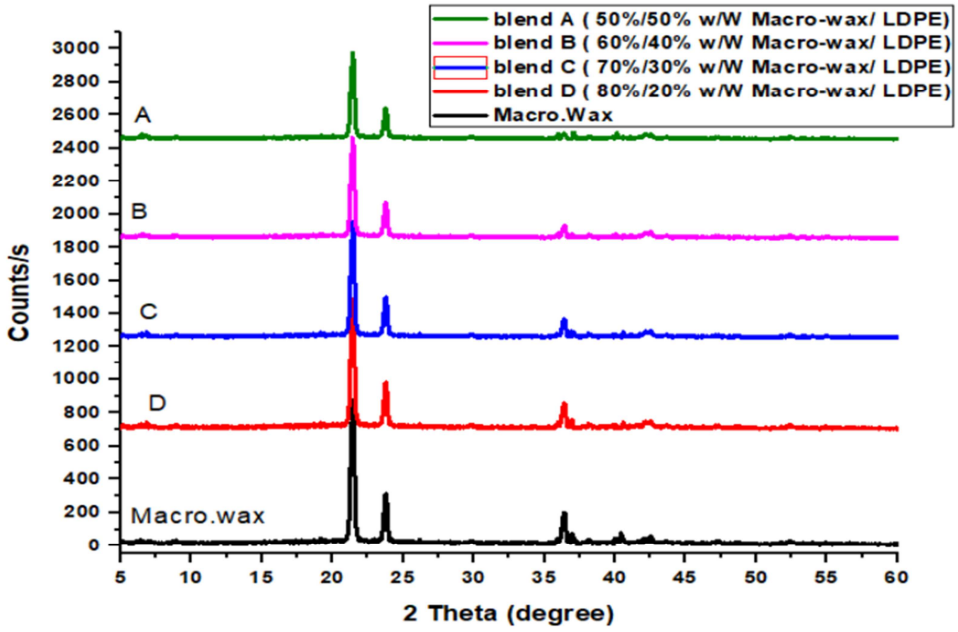

Figure 9: X-ray diffraction patterns of of macrocrystalline, macrocrystalline wax /LDPE blends

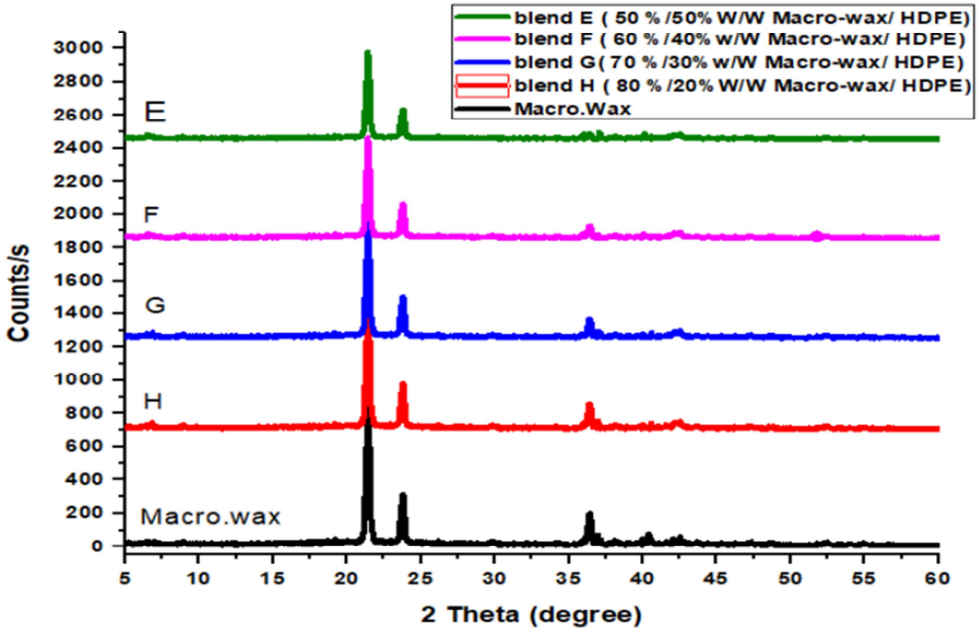

Figure 10: X-ray diffraction patterns of macrocrystalline, Macrocrystalline Wax /HDPE blends

Microcrystalline Wax Blends

Microcrystalline wax had larger, less pronounced peaks at 2θ = 21.58° and 23.96°, with no apparent peak around 36.07° (Figures 11 and 12), indicating smaller crystal domains and a higher amorphous content (crystallinity: ~61%).

Blending with LDPE or HDPE (50-80 wt% wax) resulted in little crystallinity changes (61-62%), indicating weak polymer-wax interactions. Unlike macrocrystalline wax, microcrystalline wax's disordered microstructure most likely inhibits considerable polymer-induced lattice deformation, even at high polymer ratios.

The striking contrast between macro- and microcrystalline wax mixes highlights the importance of wax morphology. Macrocrystalline wax, with its bigger, well-defined crystals, is more vulnerable to polymer-induced crystallinity suppression, whereas microcrystalline wax's intrinsic disorder mitigates these effects. Furthermore, HDPE's linear chains and higher crystallinity make it more effective in modulating wax crystallinity than branched LDPE, as shown by enhanced crystallinity recovery in HDPE blends (Figure 10 vs. 9).

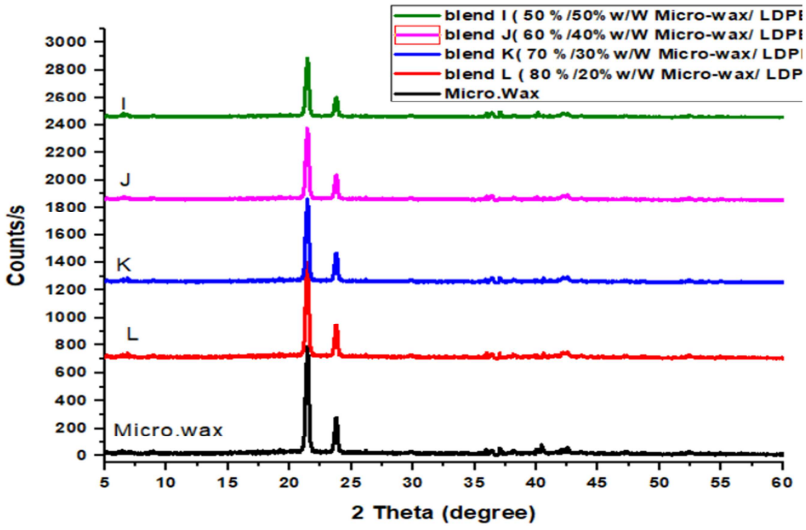

Figure 11: X-ray diffraction patterns of microcrystalline wax and microcrystalline wax/LDPE blends

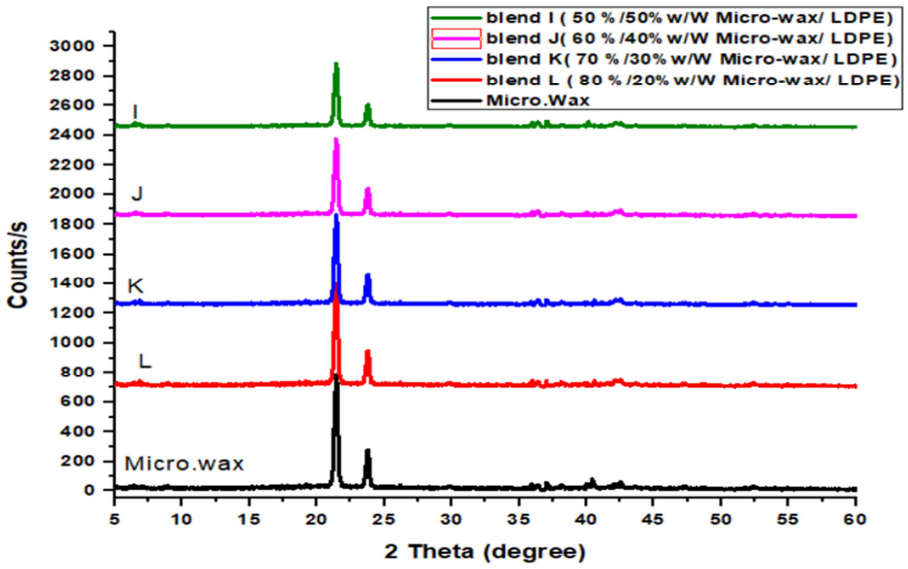

Figure 12: X-ray diffraction patterns of micro-crystalline wax and microcrystalline wax/HDPE Blends

3.1.4. The hardness of wax/polymer blends

Table 4 summarizes the congealing point and needle penetration statistics for macro and microcrystalline wax mixes containing LDPE and HDPE. A systematic drop in polymer content (50-20 wt%) was associated with a decrease in congealing point and an increase in needle penetration depth, indicating a lower blend hardness. For example, macrocrystalline wax/LDPE blends saw a congealing point fall from 92°C (50/50) to 82°C (80/20), while needle penetration increased from 3 mm to 15 mm. Similar patterns were seen for HDPE-based systems, but with slightly higher congealing points due to HDPE's intrinsic stiffness (Table 4).

Based on the analysis and measurements mentioned earlier, Macrocrystalline wax blends demonstrated superior hardness relative to microcrystalline counterparts. For example, 50/50 macrocrystalline/LDPE blends showed a needle penetration of 3 mm, compared to 5 mm for analogous microcrystalline systems. This disparity arises from macrocrystalline wax's brittle, highly ordered structure, which resists deformation under stress, whereas microcrystalline wax's amorphous-dominated morphology enhances flexibility but reduces load-bearing capacity [23,24]. These findings align with XRD and DSC data (Figures 9–12, Tables 2–3), where macrocrystalline wax blends exhibited higher crystallinity and thermal stability, further corroborating their mechanical robustness.

Table 4: The solidification temperature and needle penetration characteristics of both macro- and micro-crystalline waxes, along with their mixtures with LDPE and HDPE

Sample		Congealing point (◦C)		Needle penetration at 25◦C (mm)	
		LDPE	**HDPE**	**LDPE**	**HDPE**
Macrocrystalline wax	100/0	75		17	
	50/50 Blend	92 A	94 E	3 A	3 E
	60/40 Blend	88.5 B	89 F	4 B	4 F
	70/30 Blend	85 C	87 G	8 C	7 G
	80/20 Blend	82 D	84 H	15 D	14 H
Microcrystalline wax	**100\0**	86		20	
	50/50 Blend	97 I	99 M	5 I	5 M
	60/40 Blend	95.5 J	97 N	9 J	8 N
	70/30 Blend	93 K	95 O	14 K	13 O
	80/20 Blend	91 L	92.5 P	16 L	15 P

3.1.4. Morphological Analysis of Wax/Polymer Blends

Scanning electron microscopy (SEM) was employed to evaluate the microstructure of macrocrystalline wax blends with low- and high-density polyethylene (LDPE, HDPE). Figures 13a and 14a depict homogeneous integration of macrocrystalline wax (50/50 ratio) within the solid matrices of LDPE and HDPE, respectively. The wax phase (dark regions) is uniformly dispersed as discrete domains within the continuous polymer network (light regions), forming a cohesive composite structure. This morphological integrity prevents leakage of molten wax, a critical attribute for applications such as form-stable phase-change materials. The absence of phase separation in these blends underscores the compatibility between paraffin-based waxes and polyethylene at moderate wax concentration.

At elevated wax ratios (80/20 wt%, Figures 13b and 14b), pronounced wax domain agglomeration emerges, signaling interfacial saturation within the polymer matrix. This morphological transition reflects the limited capacity of amorphous regions in LDPE and HDPE to solubilize excess wax chains, driving wax cluster coalescence. Notably, HDPE blends develop marginally finer agglomerates than LDPE analogues—attributable to HDPE's linear chain architecture and higher crystallinity (68–85% vs. 40–60%), which restrict molecular mobility of wax constituents [25]. These findings align with DSC and XRD data (Figures 1–12, Tables 2–3), where increased wax content reduced crystallinity and enthalpic stability.

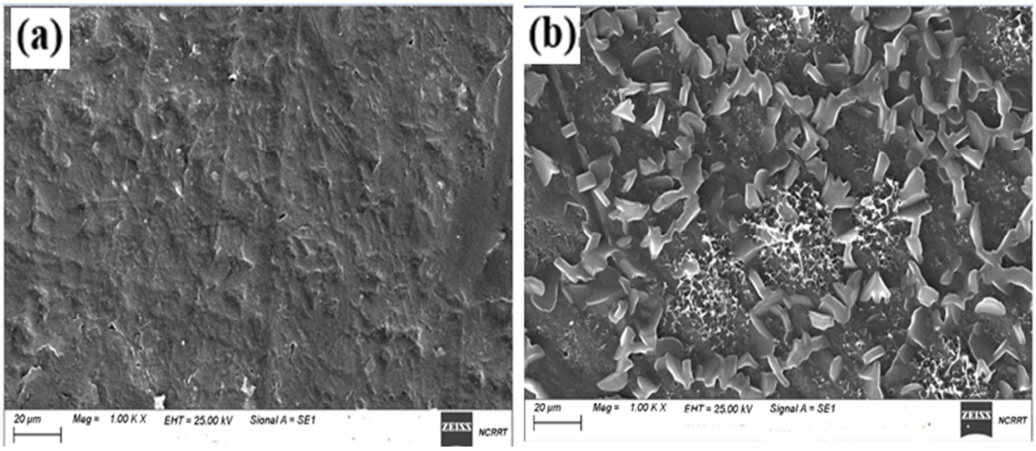

Figure 13: SEM images of macrocrystalline wax /LDPE w /w (a) 50/50 (b) 80/20

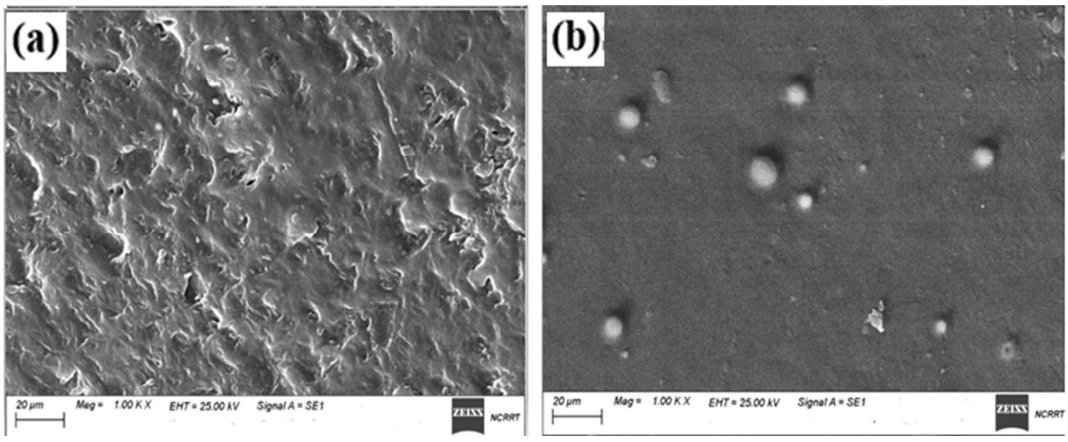

Figure 14: SEM images of macrocrystalline wax /HDPE w /w (a) 50/50 (b) 80/20

Figures 15 and 16 illustrate microcrystalline wax dispersed within LDPE and HDPE matrices. While dispersion patterns resemble macrocrystalline blends, microcrystalline wax's smaller crystal domains and amorphous-dominated structure (XRD, Figures 11–12) result in weaker interfacial adhesion. This manifests as diffuse phase boundaries and irregular wax distribution, consistent with the lower mechanical hardness observed in needle penetration tests (Table 4).

The morphological evolution of these blends is governed by the interplay of polymer architecture and wax crystallinity. LDPE's branched chains and high amorphous content facilitate wax penetration at low concentrations,

whereas HDPE's rigid, linear structure enhances encapsulation but limits wax mobility [26,27]. Macrocrystalline wax, with its ordered lattice, integrates more effectively into polymer networks compared to the disordered microcrystalline variant, which exhibits higher amorphous flexibility but reduced load-bearing capacity [28,29].

The superior structural integrity of macrocrystalline wax blends at 50–60 wt% polymer content positions them as ideal candidates for anti-scratch coatings or thermal storage materials. In contrast, microcrystalline wax systems, while mechanically softer, may suit flexible composites requiring ductility. Future studies should explore rheological and dynamic mechanical analysis to quantify structure-property relationships under operational conditions.

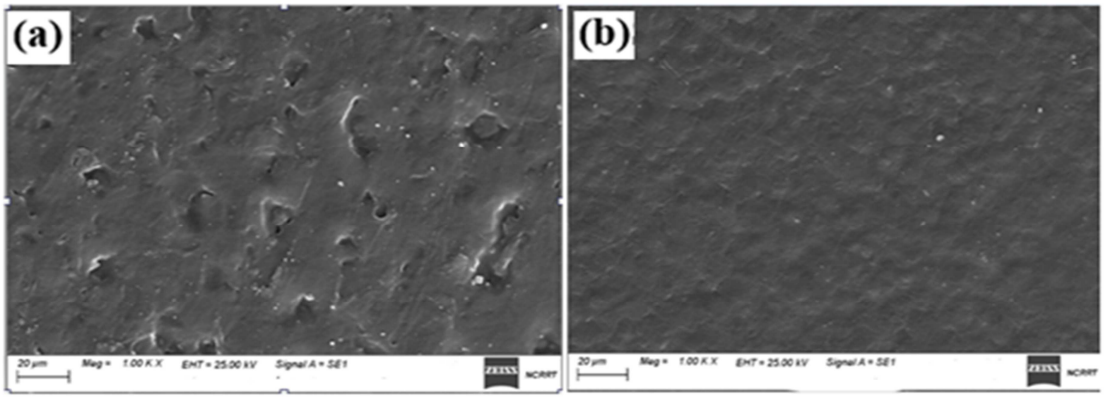

Figure 15 SEM images of microcrystalline wax /LDPE w /w(a) 50/50 (b) 80/20

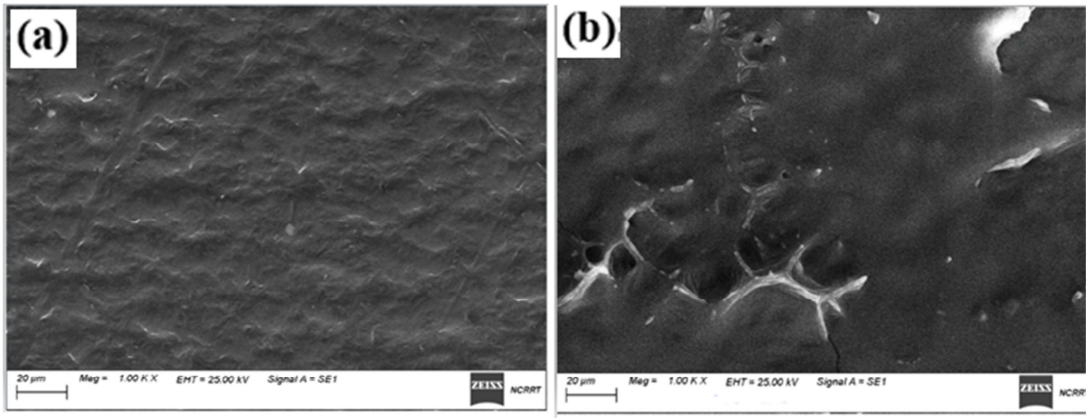

Figure 16: SEM images of microcrystalline wax /HDPE w /w (a) 50/50 (b) 80/20

3.2 Evaluations of the Ink Formulations

3.2.1 Rub Resistance

The rub resistance of ink formulations incorporating macrocrystalline wax blends with LDPE and HDPE was evaluated according to ASTM D5264, employing a 4-lb. load over 150 cycles. Visual assessments (Figure 17a–F) and quantitative rankings (Table 5) revealed distinct performance trends tied to wax type, polymer architecture, and blend ratios. representations of the prints are displayed in Figure 17 a–E.

Ink formulations with macrocrystalline wax/LDPE blends demonstrated superior rub resistance compared to wax-free controls (Figure 17a vs. 17c). Blend A (50/50 wax/LDPE) achieved a rank of 4 (near-undamaged ink layer), outperforming the control (rank 3) but falling short of the commercial benchmark (mju:wax ®2002 FN, rank 5, Figure 17b). This intermediate performance aligns with SEM observations (Figures 13a, 15a), where uniform wax dispersion within LDPE's amorphous regions enhanced mechanical integrity without fully matching commercial additives. Reducing polymer content to 60/40 (Blend B) decreased rub resistance (rank 3, Figure 17d), consistent with wax agglomeration at higher ratios (Figures 13b, 14b), which compromises interfacial adhesion.

The rub resistance trends are consistent with needle penetration data (Table 4): increasing hardness (lower penetration) was associated with better abrasion resistance. For example, Blend A's 3 mm needle penetration (Table 4)

equaled rank 4 rub resistance, but Blend E's 15 mm penetration matched rank 1. This consistency emphasizes the relationship between crystallinity, hardness, and functional performance.

Macrocrystalline wax/LDPE blends at 50–60 wt% polymer content (Blends A, B) emerge as viable candidates for anti-scratch ink formulations, balancing abrasion resistance and processability. Conversely, high-wax blends (e.g., E, F) are unsuitable due to phase-driven failures. Future work should optimize polymer-wax interfaces through compatibilizers or dynamic crosslinking to bridge performance gaps with commercial additives.

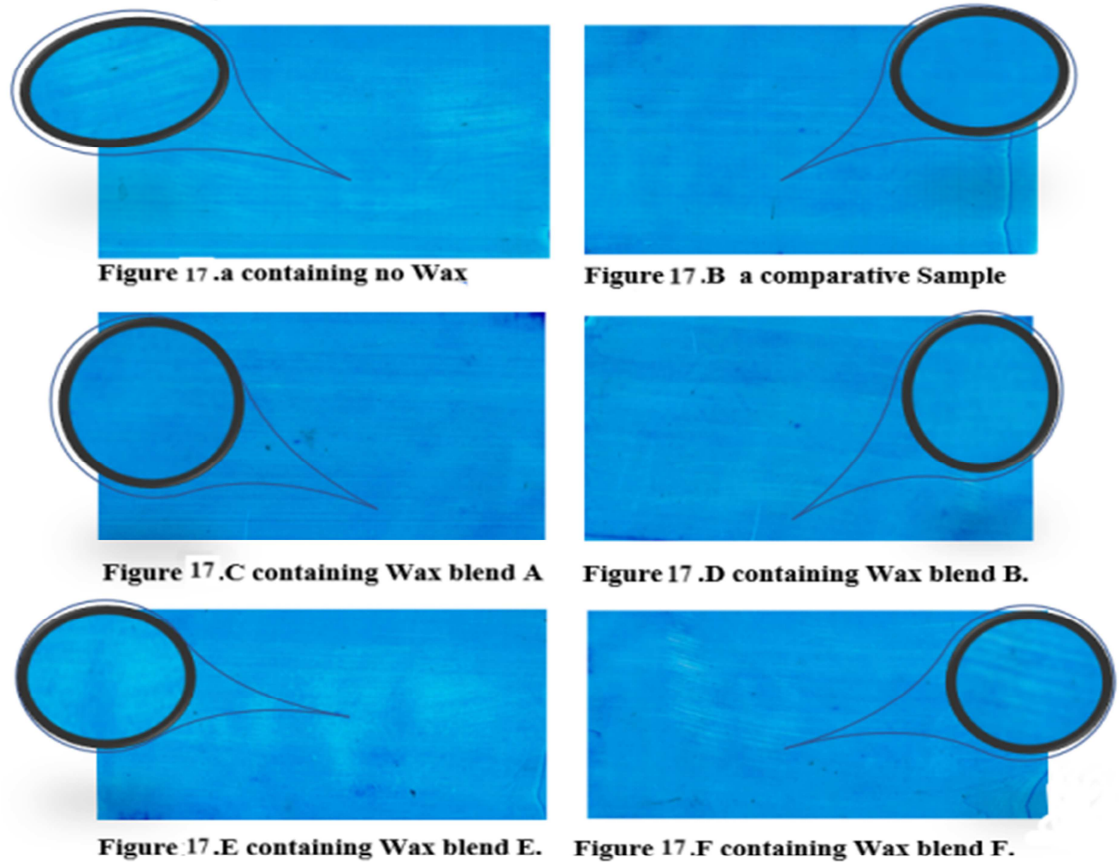

Figure 17: a -E Pictures of print's rub resistance while adding different Waxes

Table 5: Wax additives (2 wt%) on performances of ink

Sample / Test		Control	Comparative	Blends				tolerance values	standard
				A	B	E	F		
Rub resistance		3	5	4.5	4	2	1	100–200 cycles	ASTM D5264
Slip	S COF	0.45	0.36	0.38	0.39	0.45	0.41	0.3–0.6	ASTM D1894
	D COF	0.32	0.21	0.23	0.24	0.31	0.27	0.2–0.5	
Gloss (GU)		95	82	80	75	50	60	Low: 5–20 Medium: 20–50 High: 50–80+	ASTM D523

Note: 1-5 IS Rub resistance Rank Since 1 = total failure, 5 = no damage"

3.2.2 Slip Performance of Wax/Polymer Blends in Ink Formulations

The static (S COF) and dynamic (D COF) coefficients of friction for ink films, critical for packaging material processing, were evaluated using ASTM D1894. Results (Table 5) revealed distinct slip behaviours influenced by wax type, polymer matrix, and blend ratios.

The commercial benchmark (mju: wax® 2002 FN) had the lowest COF values (S COF: 0.36, D COF: 0.21) and outperformed all experimental mixes. However, Blend A (macrocrystalline wax/LDPE, 50/50 wt.%) showed comparable slip enhancement (S COF: 0.38, D COF: 0.23), reaching the market norm. Blend B (60/40 wax/LDPE) had somewhat greater friction (S COF: 0.39, D COF: 0.24), indicating less wax-polymer compatibility at lower polymer percentage. In comparison, the wax-free control had poor slip performance (S COF: 0.45, D COF: 0.32), highlighting the importance of wax additions in lowering interfacial adhesion.

Despite severe rub resistance failures (rank 1-2, Figure 17e-f), blends E and F (macrocrystalline wax/HDPE, 50/50 and 60/40 wt.%) had better slip (S COF: 0.45-0.41, D COF: 0.31-0.27) than the control. This inverse relationship demonstrates the trade-off between mechanical robustness and slip performance in HDPE-based systems. HDPE's stiff, crystalline structure (XRD, Figures 9-10), most likely limits wax dispersion, resulting in a brittle ink layer with low friction but low abrasion resistance.

Excessive COF (>0.6) can lead to web tension instability, static buildup, and creasing during packaging, while overly low COF (<0.2) risks roller slippage and uneven material flow. Blend A's balanced COF (0.38–0.23) positions it as a viable alternative to commercial additives, offering both slip enhancement and moderate rub resistance (rank 4, Table 5). The superior performance of the commercial sample likely stems from proprietary compatibilizers or optimized wax-polymer interfaces, suggesting avenues for future formulation refinement.

Slip behavior aligns with SEM observations (Figures 13–16). Homogeneous wax dispersion in LDPE blends (e.g., Blend A) reduced surface roughness and friction coefficients, whereas HDPE's crystalline domains (Figure 14a) impeded wax integration, exacerbating interfacial defects. These findings underscore the need to tailor wax/polymer ratios and architectures to optimize slip performance, mechanical durability, and thermal stability [30].

3.2.3 Impact of Wax Additives on Ink Gloss

Gloss studies, done in triplicate and averaged (Table 5), demonstrated that the introduction of wax additives into ink formulations considerably diminishes surface shine, an important aesthetic and practical feature for packaging materials. The control sample (wax-free) displayed the maximum gloss (95 GU), while wax-containing blends demonstrated gradual declines based on wax type, polymer matrix, and blend ratios.

Blend A (50/50 macrocrystalline wax/LDPE) reduced gloss by 13.7% (80 GU vs. control), closely matching the commercial benchmark (mju: wax ®2002 FN, 82 GU). This marginal decline suggests that moderate wax loading (50 wt%) preserves gloss while enhancing functional properties like rub resistance (rank 4, Table 5). Blend B (60/40 wax/LDPE), however, exhibited a more pronounced 21% reduction (75 GU), correlating with increased wax agglomeration at lower polymer content (SEM, Figures 13b, 14b), which elevates surface roughness and light scattering.

Blends E and F (50/50 and 60/40 macrocrystalline wax/HDPE) displayed severe gloss reductions of 47% (50 GU) and 36.8% (60 GU), respectively. These outcomes align with SEM observations (Figures 14b, 16b), where high wax ratios in HDPE matrices led to coarse, irregular surface morphologies due to poor wax dispersion and phase separation. The larger particle sizes of agglomerated wax domains (inferred from SEM) likely exacerbated light diffusion, further diminishing gloss.

The inverse relationship between wax content and gloss emphasizes the difficulty of reconciling practical advantages (such as slip and rub resistance) with aesthetic needs. While macrocrystalline wax/LDPE blends at 50/50 ratios (Blend A) attain a feasible equilibrium, greater wax loadings upset polymer-wax compatibility, as indicated by XRD (Figures 9–10) and DSC data (Tables 2-3), where crystallinity and enthalpic stability decrease. HDPE's stiff crystalline structure accentuates these effects, restricting wax incorporation and increasing surface flaws

For high-gloss applications (e.g., premium packaging), wax content must be optimized to ≤50 wt%, ensuring homogeneous dispersion (see SEM, Figures 13a and 14a). Blends exceeding this threshold compromise industry-accepted high-gloss standards (≥50 gloss units per ASTM D523), as observed in Blends E and F. Future formulations should investigate nanostructured wax modifications or reactive compatibilizers to suppress agglomeration and maintain surface smoothness essential for gloss retention [31].

3.3 Cost Analysis and Sustainability Benefits of Blending Macrocrystalline Wax with LDPE Wax

3.3.1. Cost Reduction Analysis

Blending macrocrystalline wax with LDPE wax at a **50:50 ratio** provides significant cost savings compared to using pure LDPE wax. Given the price differences between these materials, the potential cost reduction can be calculated as follows:

Using a 50:50 blend, the cost per kilogram of the mixture is calculated as:

Cost of Blend= (0.50×Cost of LDPE Wax) +(0.50×Cost of Macro Wax)

- Pure LDPE Wax Cost: $1.7 per kg [32],
- Macrocrystalline Wax Cost: $0.60 per kg [33].
- (mju: wax ®2002 FN) Cost: $3.4 per kg [34],

= (0.50×1.70) +(0.50×0.60) =1.15 USD per kg

Potential Cost Savings:
Compared to using LDPE wax at **$3.40 per kg**, the blended wax costs **$1.15 per kg**, resulting in a **34.8%** cost reduction. This substantial reduction in material costs makes the blend an economically viable alternative, especially for industries requiring large-scale wax consumption

3.3.2. Environmental Sustainability

Blending macrocrystalline wax with LDPE wax not only reduces production costs but also offers notable environmental benefits:

- **Waste Reduction:** Utilizing macrocrystalline wax, which is typically a waste byproduct, helps reduce industrial waste disposal and promotes a circular economy.
- **Lower Carbon Footprint:** Reducing dependency on pure LDPE wax decreases the environmental impact associated with petroleum extraction and polymer refinement.
- **Resource Conservation:** Repurposing an existing byproduct reduces the demand for virgin LDPE wax, contributing to sustainable resource utilization

4. CONCLUSIONS

The integration of recycled macro- and microcrystalline waxes—by-products of lubricating oil refining—into polymer matrices was systematically explored to develop sustainable, high-performance anti-scratch additives for flexographic inks. Key findings from DSC and TGA analyses revealed that blending low- and high-density polyethylene (LDPE, HDPE) with macrocrystalline wax significantly enhanced thermal stability and elevated melting temperatures (> 60 °C), addressing operational challenges associated with ink processing. Conversely, microcrystalline wax/polymer blends exhibited reduced hardness due to diminished crystallinity (XRD data), rendering them less suitable for scratch-resistant applications.

Notably, macrocrystalline wax/LDPE blends at 40–50 wt% polymer content demonstrated optimal performance—achieving rub resistance (rank 4), controlled slip (S COF: 0.38–0.39), and moderate gloss retention (75–80 GU), closely aligning with commercial benchmarks (e.g., *mju: wax® 2002 FN*). In contrast, HDPE-based blends suffered from brittleness and phase separation, underscoring the superior compatibility of LDPE's semi-crystalline structure with wax domains.

From a sustainability perspective, this study provides a scalable strategy for **valorizing refinery waste waxes** that would otherwise require energy-intensive disposal. Substituting 50% virgin LDPE with macrocrystalline wax reduced material costs by 33.8%, while also contributing to **material circularity**, **waste minimization**, and **carbon footprint reduction**—core targets of SDG 12. The upcycling of refinery by-products into functional additives not only conserves non-renewable petrochemical resources but also enhances the **recyclability and eco-efficiency of ink formulations**, especially in sectors like **flexible packaging**, where environmental scrutiny is growing.

The findings advance existing knowledge by demonstrating a viable pathway to **replace virgin polymers** with industrial wax waste in high-performance applications without compromising ink quality. This circular design approach contributes to a broader industrial shift toward **sustainable materials innovation** and **green chemistry solutions**. Future work should explore the incorporation of bio-based compatibilizers or nanoscale wax modifications to further decouple trade-offs between gloss, mechanical robustness, and thermal resistance. Such enhancements could expand the utility of these composites in advanced applications, including **biodegradable coatings**, **recyclable multilayer films**, and **low-carbon ink systems**.

Acknowledgement
The authors would like to extend their heartfelt thanks to the Academy of Scientific Research and Technology (ASRT) and the Scientists for the Next Generation (SNG) Program for their financial support of this research.

Reference

[1] Islam, R. U., et al. Recent developments in sustainable bio-based wax Nano emulsions as edible coatings for food commodities: A comprehensive review. *Package. Technol. Sci.* 2024, **37**(12), 1175–1194.
[2] Sayed, M. A., Elbanna, S. A., Roushdi, A. A., Hafez, E., Roushdi, M. Effect of solid contents and the ratio of EVA/Octadecyl acrylate blends on paraffin inhibition and pour point temperature of waxy crude oil. *Egypt. J. Chem.* 2022, **65**(3), 619–625.
[3] Elbanna, S. A., Abd El Rhman, A. M., Al-Hussaini, A. S., Khalil, S. A. Paraffin inhibition and pour point depression of waxy crude oil using newly synthesized terpolymeric additives. *Egypt. J. Chem.* 2022, **65**(131), 1455–1463.
[4] Wang, L., Zhang, Y., Liu, H. Structural characteristics and application potential of microcrystalline waxes in functional materials. *J. Ind. Eng. Chem.* 2021, **99**, 205–212.
[5] Kumar, A., Singh, P., Sharma, R. Advances in hydrocarbon-based waxes for industrial applications: Rheological and interfacial performance. *Prog. Org. Coat.* 2022, **165**, 106733.
[6] Zhao, Y., Tang, L., Li, X. Valorization of petroleum waste waxes: Opportunities and challenges in sustainable material development. *J. Clean. Prod.* 2020, **256**, 120446.
[7] Magazine, R., van Bochove, B., Borandeh, S., Seppälä, J. 3D inkjet-printing of photo-crosslinkable resins for microlens fabrication. *Addit. Manuf.* 2022, **50**, 102534.
[8] Yadav, D. K., et al. Experimental study on paraffin wax supported by HDPE and loaded with nano-additives. *Energies* 2024, **17**(11), 2461.

[9] Mu, M. Thermal characteristics of paraffin wax/HDPE composites as form-stable PCMs. *Res. Gate* 2023.
[10] Nabwey, H. A., Tony, M. A. Thermal energy storage using a hybrid composite based on technical grade paraffin wax. *Nanomaterials* 2023, **13**, 2635.
[11] El Sebaii, A. A., et al. Enhancing thermal properties of paraffin wax using hybrid nanomaterials. *Curr. Appl. Nanotech Nol.* 2024, **7**(1), Article 4912.
[12] Lecompte, T., et al. Form stable paraffin–Al_2O_3/HDPE composites for thermal storage. *J. Therm. Anal. Calorim.* 2020.
[13] Zhang, Y., et al. Influence of wax particle size and melting behavior on rub resistance in flexographic inks. *J. Coat. Technol. Res.* 2023, **20**(3), 455–463.
[14] Nabwey, H. A., Tony, M. A. Thermal performance and morphology of technical-grade paraffin polymer hybrid composites for industrial applications. *Nanomaterials* 2023, **13**(19), 2635.
[15] Yadav, D. K., et al. Experimental investigation of HDPE/paraffin composites for enhanced thermal energy storage and structural integrity. *Energies* 2024, **17**(11), 2461.
[16] Zhang, Y., Liu, X., Zhang, L. Valorization of refinery byproduct waxes into functional composites: A pathway toward circular and low-cost material systems. *J. Clean. Prod.* 2023, **413**, 137646.
[17] Gao, M., Liu, Y., Zhang, Z. Thermal behavior and compatibility analysis of polyethylene–wax blends using DSC and FTIR techniques. *Thermochim. Acta* 2021, **698**, 178902.
[18] Zhou, D., Wang, C., Zhang, H. Thermal analysis and phase transition behavior of paraffin/polymer composites for energy and coating applications. *J. Therm. Anal. Calorim.* 2023, **147**, 10635–10648.
[19] Sharma, R., et al. Polymer confinement effects on wax crystallization kinetics. *J. Mater. Sci.* 2021, **56**(18), 10834–10848.
[20] El Sebaii, A. A., Al Ghamdi, A. A. Effect of polyethylene type on thermal behavior of paraffin-based composites for phase change applications. *J. Therm. Anal. Calorim.* 2024, **147**, 13721–13734.
[21] Netsch N., Elsner C., Meier S., Becker M. Thermogravimetric study on thermal degradation kinetics and polymer interactions in mixed thermoplastics. *J. Therm. Anal. Calorim.* **2025**; *150*(1): 211–229.
[22] Zeng S., Lu D., Yang R. Effects of crystallinity and branched chain on thermal degradation of polyethylene. *Polym. (Basel).* **2024**; *16*(21): 3038.
[23] Mthatha L., Luyt A. S.; Thermophysical and rheological insights of polyethylene/wax blends. *Front. Chem. Eng.* **2024**, *6*, Article 1507921.
[24] Ibrahim, E. M. E., et al. Blending petroleum waxes with suitable polymeric additives as a simple and promising way to improve the quality of petroleum waxes for numerous industrial applications. *J. Pet. Sci. Technol.* 2021, **11**(2), 30.
[25] Li, Y., et al. Confinement effects on crystallization kinetics in polyethylene/wax blends. *Macromolecules* 2023, **56**(8), 3021–3032.
[26] Crystallization behavior of polyethylene blends with wax additives. *Front. Chem. Eng*. 2024, **6**, Article 1507921.
[27] El-Azab, M. M., Ebrahim, S. F., Shalaby, A. H. Effect of waste wax and chain structure on the mechanical and physical properties of polyethylene. *Arab. J. Chem.* 2023, **16**(5), 104735.
[28] Ito, A., et al. Additive effects of solid paraffins on mechanical properties of high-density polyethylene. *Polymers* 2023, **15**(5), 1320.
[29] Gupta, U., Mishra, A. K. Study of microcrystalline and macrocrystalline structure based on Cambay basin crude oils. *Upstream Oil Gas Technol.* 2022, **8**, 100067.
[30] Liang, L., et al. Investigation on the mechanical and tribological properties of polyethylene wax/silicone rubber composites. *Mater. Res. Express* 2021, **8**(9), 095306.
[31] Zhang, L., Chen, Y., Wu, J. Surface modification of wax–polymer composites for improved gloss and dispersion. *J. Appl. Polym. Sci.* 2021, **138**(22), 50342. https://doi.org/10.1002/app.50342
[32] Alibaba.com. LDPE wax price per kg. Jul. 2024. [Online]. Available: https://www.alibaba.com/showroom/polyethylene-wax-price.html
[33] Alibaba.com. Macrocrystalline paraffin wax price. Jul. 2024. [Online]. Available:
[34] https://www.alibaba.com/showroom/macrocrystalline-wax-price.html
[35] Clariant. *mju: wax® 2002 FN – Technical Data Sheet.* 2023. [Online]. Available: https://www.clariant.com